Journal of Applied Mathematics and Mechanics 73 (2009) 623–630

Contents lists available at ScienceDirect

Journal of Applied Mathematics and Mechanics

journal homepage: www.elsevier.com/locate/jappmathmech

Analysis of the steady motions of the tippe top☆

A.A. Zobova, A.V. Karapetyan

Moscow, Russia

ARTICLE INFO

Article history:
Received 23 March 2009

ABSTRACT

The motion of the tippe top on a horizontal plane is considered taking into account sliding friction within the Contensou model. The tippe top is modelled by two spherical segments rigidly joined by a rod directed along the common axis of symmetry of the segments. The dimensions of the spherical segments and the rod are chosen so that, as the axis of symmetry deviates from the upward vertical, the tippe top is supported on the plane at a point on one segment up to a certain critical value and at a point on the other segment at larger deviations (at points on both segments at the critical value). The motion of the tippe top is described by different equations in different regions of configuration space, and the motion is accompanied by impacts on the boundary of these regions. An effective potential of the system is constructed, and the type of its critical points is investigated. Poincaré–Chetayev bifurcation diagrams and generalized Smale diagrams are constructed for steady motions. Plots of the steady-state precessional motions have a discontinuity on the boundary between the regions indicated.

The tippe top (or Chinese top) consists of a spherical segment of large radius and a cylindrical shaft on the flat part of the segment. When the tippe top is supported at a point on the segment of large radius (when the shaft is pointing up), its equilibrium position is stable, but if it is spun rapidly in this position, the top quickly flips over onto the shaft. Then the rotation rate drops, and the top gradually returns to be supported at a point on the spherical segment. The stability of rotations with a vertically oriented axis of dynamical symmetry has been investigated.[1] A complete analysis of the occurrence and stability of all the steady motions based on a modified version of Routh's theory, in which the top was modelled by a dynamically symmetrical sphere with a displaced centre of mass, has been given.[2] A global qualitative investigation of the dynamics of such a model of a tippe top on a plane with sliding friction and pivoting friction has been conducted.[3] The main difference between the problem considered here and the problem previously investigated in Ref. 3 is as follows: the tippe top is modelled here by a rigid body bounded by a non-convex surface consisting of two spherical segments (the smaller segment models the shaft); the configuration space is divided into two regions, in which the motion of the body is described by different equations, and the motion on the boundary between these regions is accompanied by impacts. The method of investigation is similar to the method previously used in Ref. 3. The analytical results obtained in this paper supplement the numerical investigations of this problem performed in Ref. 4.

1. Statement of the problem

Consider a heavy rigid body on a horizontal plane. The body (which we will call a top) consists of two spherical segments with radii r_1 and r_2, which complement one another in the sense that while the first segment is formed by rotating a $2(\pi - \alpha)$ arc of a circle about the axis of symmetry, the other is formed by rotating a 2α arc. The two segments are rigidly joined by a rod that passes through their centres O_1 and O_2 (Fig. 1).

The geometrical parameters of the top α, r_1, r_2 and l (l is the distance between the centres of the segments O_1 and O_2) are related by the expression

$$l = (r_1 - r_2)/\cos\alpha$$

☆ *Prikl. Mat. Mekh.* Vol. 73, No. 6, pp. 867-877, 2009.
E-mail address: azobova@mail.ru (A.A. Zobova).

0021-8928/$ – see front matter
doi:10.1016/j.jappmathmech.2010.01.001

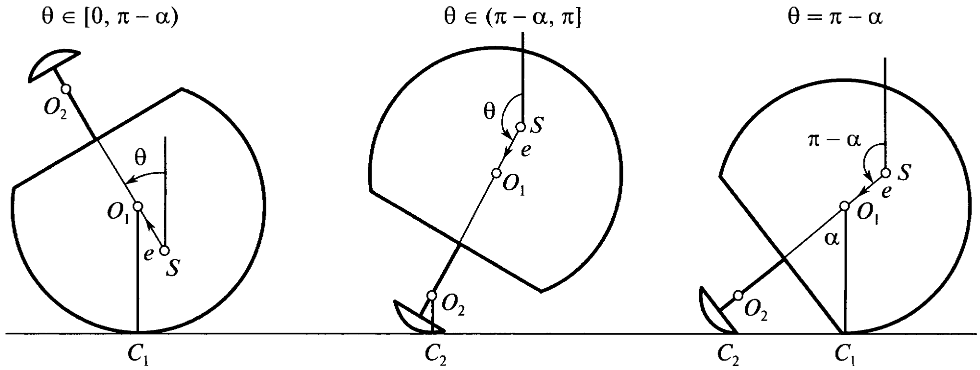

Fig. 1.

To be specific, we will assume that $r_1 > r_2$ and that $\alpha \in (0, \pi/2)$. The top is then supported on the horizontal plane at a point on the first spherical segment if $\theta \in [0, \pi - \alpha)$ and at a point on the other spherical segment if $\theta \in (\pi - \alpha, \pi]$, and the top is supported on the plane at two points if $\theta = \pi - \alpha$. Here θ is the angle of deviation of the axis of symmetry (the rod) from the upward vertical.

Let the centre of mass S of the top lie on its geometrical axis of symmetry O_1O_2 at a distance c_1 from the point O_1 outside of the segment O_1O_2. Then $O_2S = c_2 = l + c_1$. We will assume that this axis is also the axis of dynamic symmetry of the top, and we will use $J_1, J_2 = J_1$ and J_3 to denote the principal central moments of inertia of the top and m to denote its mass.

We introduce the dimensionless parameters of the top

$$\alpha \in (0, \pi/2), \quad b_1 = c_1/r_1 \in (0, 1), \quad b_2 = c_2/r_2 \in (1, +\infty)$$
$$a = J_1/J_3 \in [1/2, +\infty)$$

Here

$$\frac{r_2}{r_1} = \frac{1 + b_1\cos\alpha}{1 + b_2\cos\alpha} < 1, \quad \frac{l}{r_1} = \frac{b_2 - b_1}{1 + b_2\cos\alpha} > 0$$

Let $\mathbf{e} = \overline{O_1O_2}/O_1O_2$ be the unit vector of the axis of symmetry of the top, $\boldsymbol{\gamma}$ the unit vector of the upward vertical, $\mathbf{v}$ the velocity of the centre of mass of the top, and ω its angular velocity. We will denote $\cos\theta = (\mathbf{e}, \boldsymbol{\gamma})$ by $x \in [-1, 1]$. When $x \in \Delta_1 = (-\cos\alpha, 1]$, the top is supported on the plane at a point on the first segment, and when $x \in \Delta_2 = [-1, -\cos\alpha)$, it is supported at a point on the other segment. Let $C = C_1$ be the point of support on the plane ($i = 1$ if $x \in \Delta_1$, and $i = 2$ if $x \in \Delta_2$). Then

$$\mathbf{r}_i = \overrightarrow{SC} = -r_i\gamma + c_i\mathbf{e} = -r_i(\gamma - b_i\mathbf{e}), \quad i = 1, 2$$

2. The equations of motion of the top and their properties

Assuming that, in addition to the normal reaction, dry friction forces act on the top at its point of support on the plane within the Contensou model (i.e., neglecting the pivoting friction torque), we write the equations of motion of the top relative to its principal central axes of inertia

$$m\dot{\mathbf{v}} + [\boldsymbol{\omega}, m\mathbf{v}] = (N - mg)\boldsymbol{\gamma} + \mathbf{F}, \quad \mathbf{J}\dot{\boldsymbol{\omega}} + [\boldsymbol{\omega}, \mathbf{J}\boldsymbol{\omega}] = [\mathbf{r}, N\boldsymbol{\gamma} + \mathbf{F}]$$
$$\dot{\boldsymbol{\gamma}} + [\boldsymbol{\omega}, \boldsymbol{\gamma}] = 0, \quad (\mathbf{v} + [\boldsymbol{\omega}, \mathbf{r}], \boldsymbol{\gamma}) = 0 \tag{2.1}$$

where $\mathbf{J} = \mathrm{diag}(J_1, J_1, J_3)$ is the central tensor of inertia of the top, N is the normal reaction at the point of support and $\mathbf{F}$ is the force of sliding friction.

The first equation in (2.1) expresses the theorem of momentum of the top, the second equation expresses the theorem of angular momentum about the centre of mass, the third equation expresses the condition of constancy of the vector $\boldsymbol{\gamma}$ in the absolute frame of reference, and the fourth equation expresses the condition of motion of the sphere without bouncing. If the friction force is specified in the form $\mathbf{F} = \mathbf{F}(\mathbf{v}, \omega, \boldsymbol{\gamma}, N)$, system (2.1) is closed with respect to the variables $\mathbf{v}$, ω, $\boldsymbol{\gamma}$ and N.

Equations (2.1) describe the motion of the top when $x \neq -\cos\alpha$: if $x \in \Delta_i$, then $N = N_i$, $\mathbf{r} = \mathbf{r}_i$, and $\mathbf{F} = \mathbf{F}_i$ ($i = 1, 2$). When $x = -\cos\alpha$, the right-hand sides of the first two equations in (2.1) should be changed, respectively, to

$$-mg\gamma + \sum_{i=1}^{2}(N_i\gamma + \mathbf{F}_i), \quad \sum_{i=1}^{2}([\mathbf{r}_i, N_i\gamma + \mathbf{F}_i]$$

and the single last equation in (2.1) (for $i = 1$ or $i = 2$) should be replaced by two such equations (for $i = 1$ and $i = 2$).

Let $x \neq -\cos\alpha$. Then the sliding velocity of the top is specified by the relation $\mathbf{u} = \mathbf{v} + [\omega, \mathbf{r}]$ ($\mathbf{r} = \mathbf{r}_i$ for $x \in \Delta_i$, $i = 1, 2$). In this case[1,5] $(\mathbf{F}, \mathbf{u}) < 0$ if $\mathbf{u} \neq 0$, and $\mathbf{F} = 0$ if $\mathbf{u} = 0$. Thus, the total mechanical energy of the top is the non-increasing function

$$H = \frac{1}{2}m\mathbf{v}^2 + \frac{1}{2}(\mathbf{J}\omega, \omega) - mg(\mathbf{r}, \gamma), \quad \dot{H} = (\mathbf{F}, \mathbf{u}) \le 0 \tag{2.2}$$

where the energy H is constant in motions without sliding and decreases in motions with sliding.

Consider the "normalized" projection K of the angular momentum $\mathbf{J}\omega$ of the top onto the radius vector $\mathbf{r}$ of its point of support on the plane (when $x \neq \cos\alpha$)

$$K = -\frac{1}{r}(\mathbf{J}\omega, \mathbf{r})$$

and its derivative with respect to time by virtue of system (2.1)

$$\dot{K} = 0 \tag{2.3}$$

Hence it follows that Jellett's integral exists

$$K_i = k_i = \text{const}, \quad i = 1, 2 \tag{2.4}$$

for $x \neq \cos\alpha$ in the corresponding region $x \in \Delta_i$ ($i = 1, 2$) of the Poisson sphere $S^2 = \{\gamma \in \mathbb{R}^3 : \gamma^2 = 1\}$.

Now suppose that $x = -\cos\alpha$ (in this case $(\mathbf{r}_1, \boldsymbol{\gamma}) = (\mathbf{r}_2, \boldsymbol{\gamma})$). Then formulae (2.2) and (2.3) take the form

$$\dot{H} = \sum_i (\mathbf{F}_i, \mathbf{u}_i), \quad \dot{K}_i = -\frac{1}{r_i}\sum_j (\mathbf{r}_i, [\mathbf{r}_j, N_j\gamma + \mathbf{F}_j]); \quad i, j = 1, 2; \quad i \neq j \tag{2.5}$$

Thus, when $x = -\cos\alpha$, there are no integrals of the form (2.4): $\dot{K}_i \neq 0$ ($i = 1, 2$). In this case (see the second equation in (2.1)) we have

$$r_1\dot{K}_1 - r_2\dot{K}_2 = r_1 r_2 (b_2 - b_1)([\gamma, \mathbf{e}], \mathbf{F}_1 + \mathbf{F}_2)$$

3. Analysis of the dynamics of the tippe top

For all $x \neq -\cos\alpha$ we can introduce the effective potential[2,3,6]

$$V = \min_{\mathbf{v},\omega} H(\mathbf{v}, \omega, \gamma)|_{K(\omega,\gamma)=k} = V(\gamma, k)$$

It has the form[3]

$$V(\gamma, k) = mgr - mgc(\gamma, \mathbf{e}) + \frac{k^2}{2J(\gamma)}; \quad J(\gamma) = (\mathbf{J}(\gamma - b\mathbf{e}), (\gamma - b\mathbf{e}))$$

and is defined on the Poisson sphere S^2 with the exception of the parallel $(\boldsymbol{\gamma}, \mathbf{e}) = -\cos\alpha$. Here, as above, all the quantities that are defined for $x = (\boldsymbol{\gamma}, \mathbf{e}) \in \Delta_i$ have the subscripts $i = 1, 2$.

Thus, the effective potential $V(\gamma, k)$ is specified in different parts of the Poisson sphere by different formulae:

$$V = V_i = mgr_i[1 + b_i f_i(x, k_i)], \quad x \in \Delta_i$$

$$f_i = -x + \frac{k_i^2}{2J_3 mgc_i[a(1 - x^2) + (x - b_i)^2]}$$

According to a modified version of Routh's theory,[2] the critical points of the functions $f_i(x)$: $\Delta_i \to \mathbb{R}$ correspond to steady motions of the top: the minimum points correspond to stable motions, and the maximum points correspond to unstable motions.[3]

The functions f_1 and f_2 always have the critical points at $x = 1$ and $x = -1$, respectively, which correspond to uniform rotations of the top about the vertically oriented axis of symmetry (at $x = 1$ the top is supported on the plane at a point on the spherical segment of larger radius, and at $x = -1$ it is supported at a point on the spherical segment of smaller radius), and at the corresponding values of the parameter k_i (the constant of the Jellett's integral) the critical points $x_0 \in (-1, 1)$, which correspond to precessional motions of the top. The latter are determined from the equation $f_i'(x) = 0$, which can be represented in the form

$$p_i^2 = \frac{k_i^2}{J_3 mgc_i} = \frac{[a(1 - x^2) + (x - b_i)^2]^2}{b_i - (1 - a)x} = \varphi_i(x) \tag{3.1}$$

The character of the critical points $x = \pm 1$, as well as the number and character of the critical points $x_0 \in (-1, 1)$ that satisfy Eq (3.1), depend significantly both on the parameters a and b_i of the top and on the values of p_i^2. (Note that the functions $\varphi_i(x)$ were determined in the intervals Δ_i, respectively.) We will next provide a detailed description of the investigation of the behaviour of the functions $\varphi_i(x)$ in relation to the parameters (for simplicity, we will temporarily omit the subscript i).

4. Investigation of equation of precessional motions

We first note that since a non-negative quantity appears on the left-hand side of Eq. (3.1), precessional motions occur only in the part of the interval $[-1, 1]$ where the function $\varphi(x)$ takes non-negative values. The equation of the asymptote of the function $\varphi(x)$ is $x = x_{as} = b/(1 - a)$. The asymptote lies in the band $\Delta_1 \times \mathbb{R}$ if $b < \cos\alpha\,(a - 1)$ (then $x_{as} < 0$, and the function $\varphi(x)$ takes positive values for $x_{as} < x < 1$) or if $b < 1 - a$ (in this case $x_{as} > 0$, and the function $\varphi(x)$ takes positive values for $-1 < x < x_{as}$). The asymptote lies in the band $\Delta_2 \times \mathbb{R}$ if $\cos\alpha\,(a - 1) < b < a - 1$ (and $\varphi(x) > 0$ for $x_{as} < x < \cos\alpha$). If $b < \cos\alpha\,(a - 1)$, the function $\varphi(x)$ takes negative values over the entire interval Δ_2; if $b < a - 1$, the function $\varphi(x)$ is positive over the entire interval Δ_2.

We will investigate the nature of the monotonicity of the function $\varphi(x)$. The derivative of this function has the form

$$\varphi'(x) = \frac{a(1-x^2)+(x-b)^2}{(b-(1-a)x)^2}y(x)$$
$$y(x) = -3(1-a)^2x^2 + 6b(1-a)x + (a - ab^2 - 3b^2 - a^2)$$

It is clear that the first factor is always positive in the interval $(-1, 1)$. Consider the behaviour of the factor $y(x)$ in this interval. The graph of the function $y(x)$ is a parabola, whose branches are directed downward, with apex at the point x_{as}. Note that $y(x_{as}) = a(1 - a - b^2)$. Consequently, for values of the parameters that obey the inequality $a > 1 - b^2$, the function $y(x)$ is negative on the entire number axis, and the function $\varphi(x)$, therefore, decreases monotonically.

Next, suppose that $x_{as} > 1$, i.e., $1 - b < a < 1$. Then $y(x) < 0$ over the entire interval $(-1, 1)$ if $y(1) < 0$. It has one root $x_* \in \Delta_1$ if $y(1) > 0$ and $y(-\cos\alpha) < 0$ (then $y(x) < 0$ for $x < x_*$ and $y(x) > 0$ for $x > x_*$; therefore, x_* corresponds to the minimum of the function $\varphi(x)$). Conversely, $y(x) > 0$ over the entire interval Δ_1 if $y(1) > 0$ and $y(-\cos\alpha) < 0$. The values of $y(1)$ and $y(-\cos\alpha)$ depend on a and b:

$$y(1) = -4a^2 + (1-b)(7+b)a - 3(1-b)^2$$
$$y(-\cos\alpha) = -3(1-a)^2\cos^2\alpha - 6b(1-a)\cos\alpha + (a - ab^2 - 3b^2 - a^2)$$

In the (b, a) plane the $y(1) = 0$ and $y(-\cos\alpha) = 0$ curves pass through the point $a = 1$, $b = 0$ and have the common tangent $a = 1$ in it. It is also clear that the $y(-\cos\alpha) = 0$ curve in the region $a > 1 - b$ on the (b, a) plane always lies below the branch of the $y(1) = 0$ curve passing through this region.

Now consider the region of parameters $1/2 < a < 1 - b$. In this case the apex of the parabola $y = y(x)$ is at the following location: $0 < x_{as} < 1$. The function $y(x)$ changes sign at a certain point $x_* \in (-\cos\alpha, x_{as})$ if $y(-\cos\alpha) < 0$, since we always have $y(x_{as}) = a(1 - a - b^2) > 0$ in this parameter region. In this case $y(x)$ increases in the interval $(-\cos\alpha, x_{as})$ and x_* is the minimum point of the function $\varphi(x)$.

The properties of the functions $\varphi_i(x)$ just described enable us to demarcate the regions $\Omega_a, \Omega_b, \ldots \Omega_g$ on the plane of parameters (b_1, a) of the top (Fig. 2). In the region Ω_a the function $\varphi_1(x)$ is positive and decreases in the interval $(b_1/(1 - a), 1]$, and $\varphi_1(x) \to +\infty$ as $x \to b_1/(1 - a)$. In the region Ω_b the function $\varphi_1(x)$ is positive and decreases at $x \in \Delta_1$. In the regions Ω_c and Ω_d we have $\varphi_1(x) > 0$ when $x \in \Delta_1$, and $\varphi_1(x)$ has a minimum at the point x_*. In addition, $\varphi(1) > \varphi(-\cos\alpha)$ in the region Ω_c, and $\varphi(1) < \varphi(-\cos\alpha)$ in the region Ω_d. These regions are separated by the curve

$$\varphi(1) = \frac{(1-b)^4}{a-(1-b)} = \frac{\left[a\sin^2\alpha + (\cos\alpha + b)^2\right]^2}{b + (1-a)\cos\alpha} = \varphi(-\cos\alpha)$$

In the region Ω_e the function $\varphi_1(x)$ is positive and increases monotonically when $x \in \Delta_1$. In the regions Ω_f and Ω_g the function $\varphi_1(x)$ is positive in the interval $(-\cos\alpha, b_1/(1 - a))$ and tends to infinity as $x \to b_1/(1 - a)$. In addition, in the region Ω_f the function $\varphi_1(x)$ is monotonic, and in the region Ω_g it has a minimum at x_*. The regions Ω_i, Ω_j, and Ω_h are demarcated on the (a, b_2) parameter plane (Fig. 3). We have $\varphi_2(x) > 0$ in the region Ω_i when $x \in (b_2/(1 - a), -\cos\alpha]$ and in the region Ω_j when $x \in \Delta_2$ (this function is monotonic in these intervals), and $\varphi_2(x) \to +\infty$ as $x \to b_2/(1 - a)$ in the region Ω_i. In the region Ω_h we have $\varphi_2(x) < 0$ when $x \in \Delta_2$.

The next section qualitatively describes the generalized Poincaré–Chetayev and Smale bifurcation diagrams for each of the separate regions.

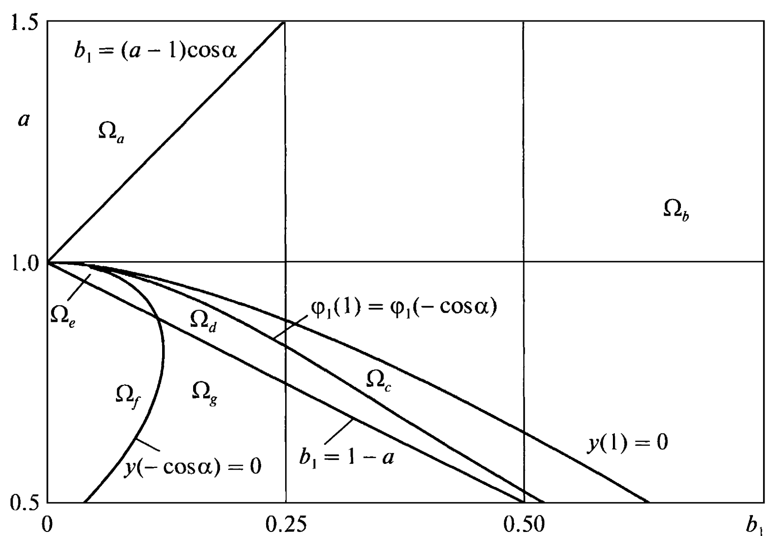

Fig. 2.

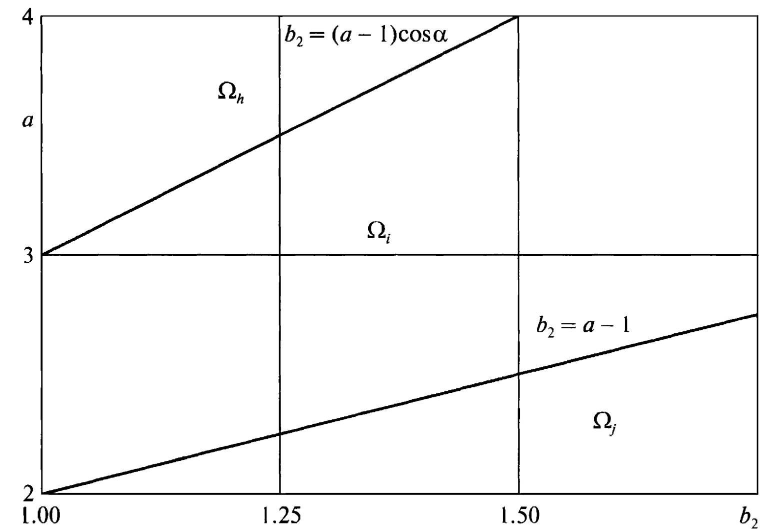
4
a
3
2
1.00
1.25
1.50
b_2
$b_2 = (a-1)\cos\alpha$
Ω_h
Ω_i
$b_2 = a - 1$
Ω_j

Fig. 3.

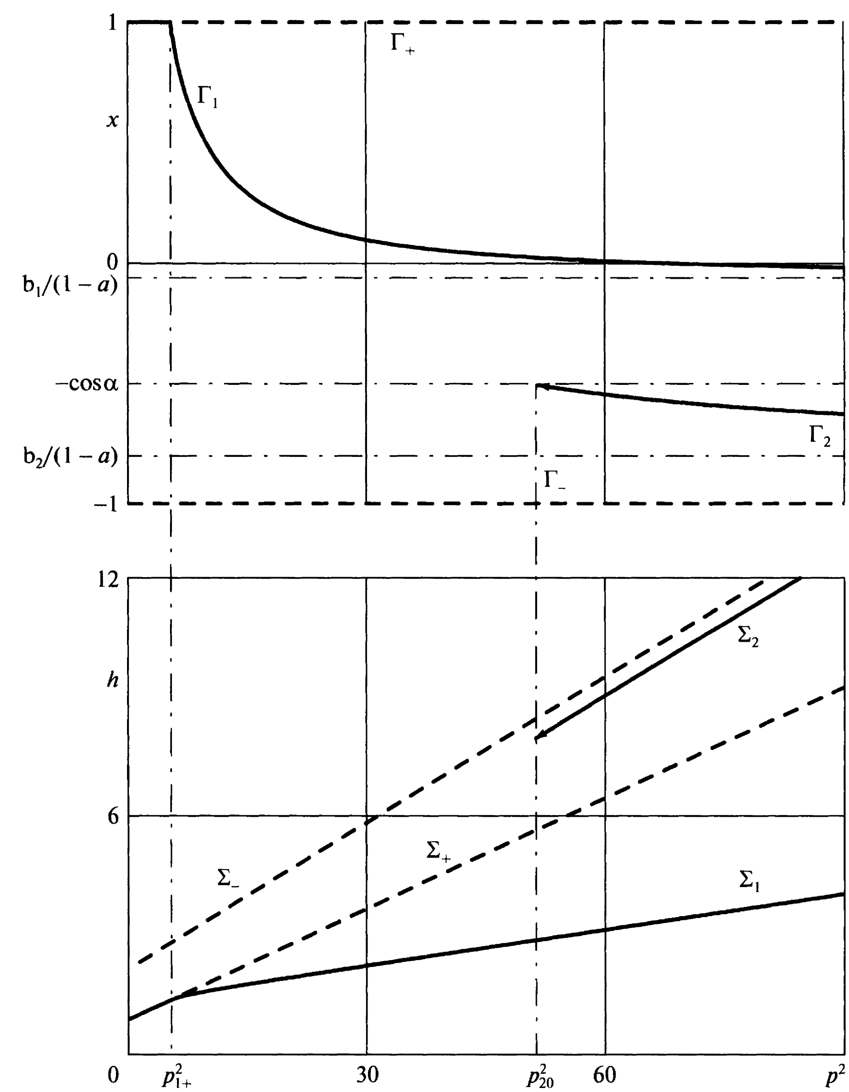
1
x
0
$b_1/(1-a)$
$-\cos\alpha$
$b_2/(1-a)$
−1
Γ_+
Γ_1
Γ_2
Γ_-
12
h
6
0
p_{1+}^2
30
p_{20}^2
60
p^2
Σ_2
Σ_-
Σ_+
Σ_1

Fig. 4.

5. Bifurcation diagrams

We will examine the generalized Poincaré–Chetayev and Smale bifurcation diagrams for the two-sphere top. Graphs of the precessional motions $x = (\boldsymbol{\gamma}, \mathbf{e}) \equiv$ const, specified by Eq. (3.1) (denoted by Γ_1 and Γ_2), as well as the straight lines of the uniform rotations $\Gamma_+ = \{x = 1\}$ and $\Gamma_- = \{x = 1\}$, are constructed as functions of the values of Jellett's integrals p_i^2 on the Poincaré–Chetayev diagrams. The thick solid lines indicate stable motions, and the thick dashed lines indicate unstable motions. Note that on the Poincaré–Chetayev diagrams each of the intervals Δ_i has its own value of the constant p_i^2.

On the generalized Smale diagrams (in the (p^2, h) plane, where h is the initial value of the total mechanical energy), the uniform rotations at $x = \pm 1$ correspond to the straight lines

$$\Sigma_\pm : h = h_i^\pm = mgr_i[1 + b_i f_i(\pm 1, p_i)]$$

The precessional motions correspond to curves that are parametrically specified by the relations

$$\Sigma_i : h = h_i = mgr_i[1 + b_i f_i(x_i, p_i)], \quad p^2 = p_i^2 = \varphi_i(x_i)$$

(x_i is a parameter that can be eliminated).

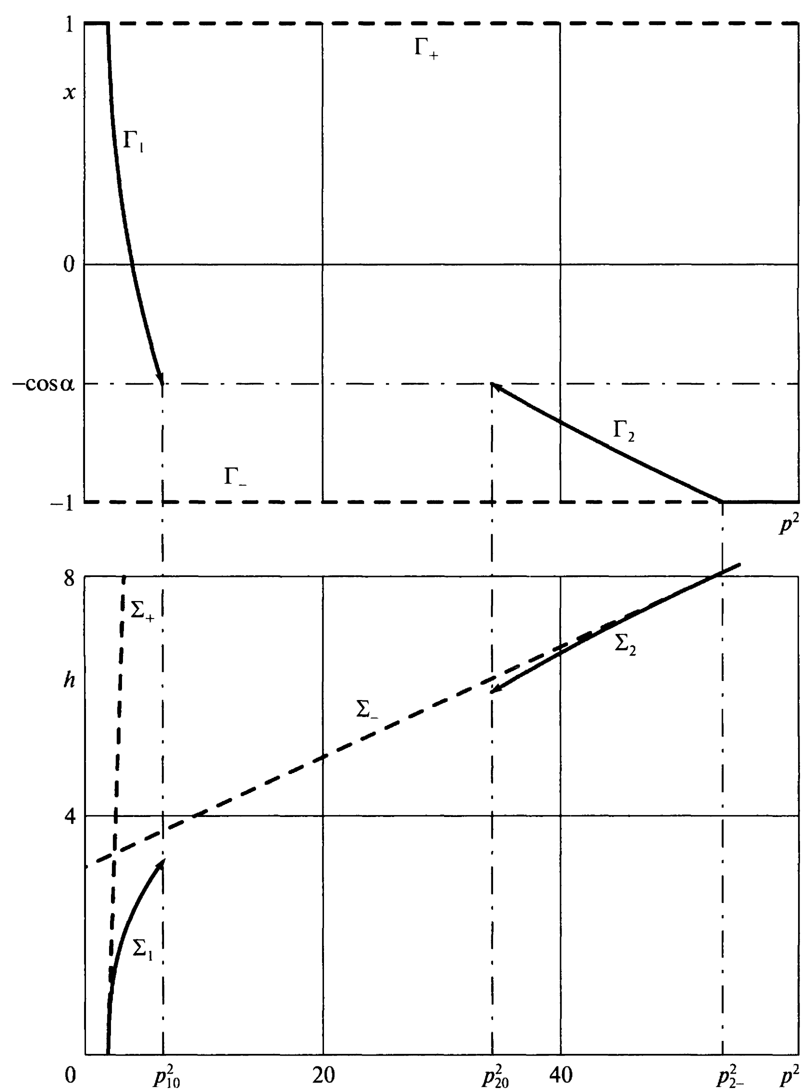

Fig. 5.

For convenience in the ensuing presentation, we also introduce the following quantities

$$p_{i+}^2 = \varphi_i(1) = \frac{(1 \mp b_i)^4}{b_i \pm (a-1)}$$

$$p_{i0}^2 = \varphi_i(-\cos\alpha) = \frac{\left[a\sin^2\alpha + (\cos\alpha + b_i)^2\right]^2}{b_i + (a-1)\cos\alpha}; \quad i = 1, 2$$

$$x_* = \frac{\sqrt{3}b_1 - \sqrt{a - ab_1^2 - a^2}}{1-a}, \quad p_*^2 = \varphi_1(x_*)$$

(x_* is the minimum point of the function $\varphi_1(x)$ in the interval Δ_1).

We will give a qualitative description of the diagrams for each of the parameter regions specified. The most interesting diagrams are presented in the figures.

1. *The case* when $(a, b_1) \in \Omega_a$, $(a, b_2) \in \Omega_i$ (Fig. 4). The uniform rotations at the lowest position of the centre of mass Γ_+ are stable only for small values of the angular velocity ($p_1^2 < p_{1+}^2$). At the point of loss of stability, the precession curve Γ_1 branches off from Γ_+ and then tends monotonically to the horizontal asymptote $x = x_{as}$; precessional motions with support at a point on the segment of large radius occur when $x \in (b_1/(1-a), 1)$ and are always stable. The uniform rotations at the highest position of the centre of mass Γ_- are unstable. Precessional motions with support at a point on the segment of small radius (curve Γ_2, which has a horizontal asymptote) occur when $x \in (-\cos\alpha, b_2/(1-a))$ and are always stable.
2. *The case* when $(a, b_1) \in \Omega_b$, $(a, b_2) \in \Omega_j$ (Fig. 5). The uniform rotations at the lowest position of the centre of mass Γ_+ are only stable for small values of the angular velocity ($p_1^2 < p_{1+}^2$). At the point of the loss of stability, the precession curve Γ_1 branches off from Γ_+ and then continues when $p_{1+}^2 < p_2^2 < p_{10}^2$. All the precessional motions when $x \in \Delta_1$ are stable. The uniform rotations at the highest

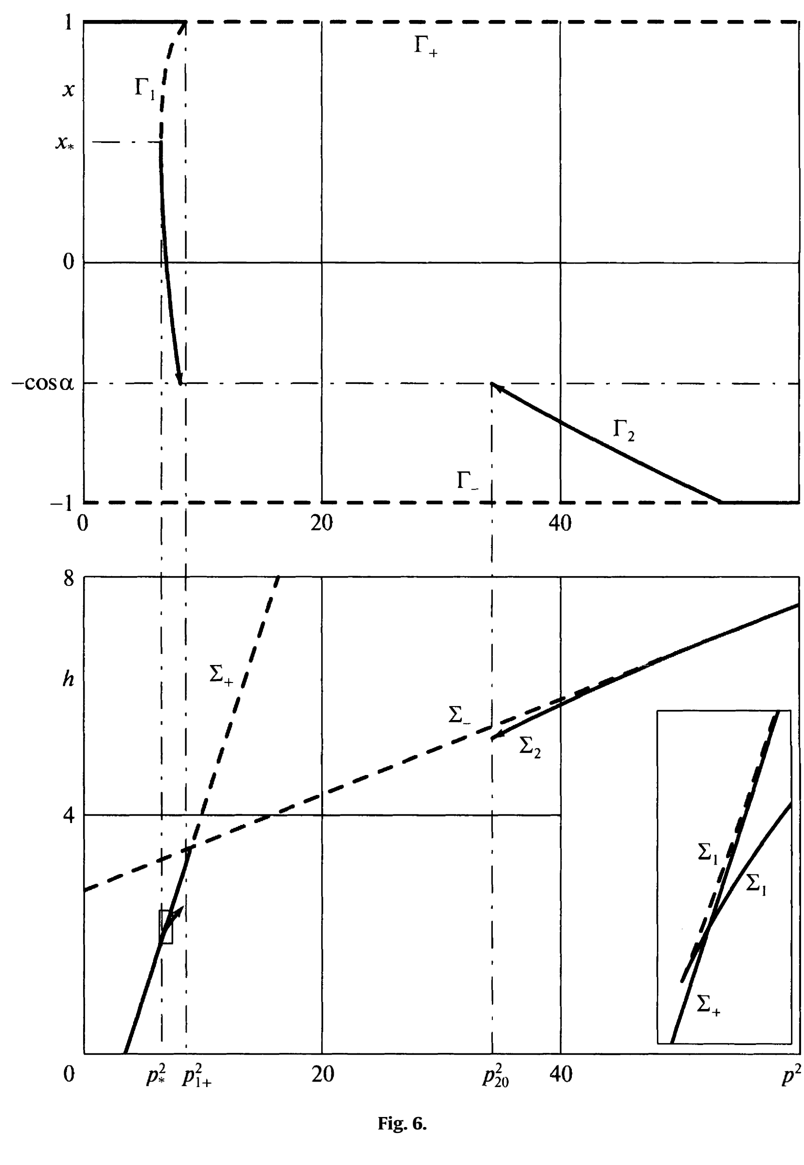

Fig. 6.

position of the centre of mass Γ_- are stable for large values of the angular velocity ($p_2^2 > p_{2-}^2$). The precessional motions when $x \in \Delta_2$ (curve Γ_2) occur when $p^2{}_{20} < p_2{}^2 < p^2{}_{2-}$ and are always stable.

3. *The case* when $(a, b_1) \in \Omega_a$, $(a, b_2) \in \Omega_j$. The properties of the diagrams in the Δ_1 part are the same as in Case 1. The properties of the diagrams in the Δ_2 part are the same as in Case 2.
4. *The case* when $(a, b_1) \in \Omega_a$, $(a, b_2) \in \Omega_h$. The properties of the diagrams in the Δ_1 part are the same as in Case 1. The uniform rotations at the highest location of the centre of mass Γ_- are always unstable. There are no precessional motions with support at a point on the spherical segment of small radius in the top.
5. *The case* when $(a, b_1) \in \Omega_b$, $(a, b_2) \in \Omega_i$. The properties of the diagrams in the Δ_1 part are the same as in Case 2. The properties of the diagrams in the Δ_2 part are the same as in Case 1.
6. *The case* when $(a, b_1) \in \Omega_d$, $(a, b_2) \in \Omega_j$ (Fig. 6). The uniform rotations at the lowest position of the centre of mass Γ_+ are only stable for small values of the angular velocity ($p_1{}^2 < p^2{}_{1+}$). At the point of the loss of stability, the precession curve Γ_1 branches off from Γ_+ and then continues when $p_*^2 < p_1^2 < p_{1+}^2$. For each value Jellett's integral p_1^2 from the interval ($p_*{}^2 < p^2{}_{10}$), there are two precessional motions, one of which is stable, and the other is not. The precessional motions are stable for $x_* < x < -\cos\alpha$. Here and in all the following cases the properties of the diagrams in the Δ_2 part are the same as in Case 2.
7. *The case* when $(a, b_1) \in \Omega_c$, $(a, b_2) \in \Omega_j$. The uniform rotations at the lowest position of the centre of mass Γ_+ are only stable for small values of the angular velocity ($p_1^2 < p_{1+}^2$). At the point of loss of stability, the precession curve Γ_1 branches off from Γ_+ and then continues when $p_*^2 < p_1^2 < p_{10}^2$. For each value of Jellett's integral p_1^2 from the interval ($p_*^2 < p_{1+}^2$), there are two precessional motions, one of which is stable, and the other is not. The precessional motions are stable when $x_* < x < -\cos\alpha$.
8. *The case* when $(a, b_1) \in \Omega_e$, $(a, b_2) \in \Omega_j$. The uniform rotations at the lowest position of the centre of mass Γ_+ are stable only for small values of the angular velocity ($p_1^2 < p_{1+}^2$). At the point of loss of stability, the precession curve Γ_1 branches off from Γ_+ and then continues when $p_{10}^2 < p_1^2 < p_{1+}^2$. All the precessional motions are unstable.
9. *The case* when $(a, b_1) \in \Omega_f$, $(a, b_2) \in \Omega_j$. The uniform rotations at the lowest position of the centre of mass are always stable. Precessional motions occur when $p_1^2 > p_{10}^2$, where $-\cos\alpha < x < b_1/(1-a)$, and the curve Γ_1 tends monotonically to the horizontal asymptote. All the precessional motions are unstable.
10. *The case* when $(a, b_1) \in \Omega_g$, $(a, b_2) \in \Omega_j$. The uniform rotations at the lowest position of the centre of mass are always stable. Precessional motions occur when $p_1^2 > p_*^2$, where $-\cos\alpha < x < b_1/(1-a)$, and the curve Γ_1 tends monotonically to the horizontal asymptote. The precessional motions are stable when $x_* < x < -\cos\alpha$.

Note that in the problem considered the graphs of the precessional motions on the Poincaré–Chetayev and Smale bifurcation diagrams are discontinuous, unlike the analogous diagrams in the simpler problem of the motion of a tippe top bounded by a spherical surface.[3] This is because there are precessional motions for different values of the constant of Jellett's integral p^2 and the energy h when $\theta = \pi - \alpha - 0$ and $\theta = \pi - \alpha + 0$.

Acknowledgements

We thank F. L Chernous'ko for drawing our attention to Ref. 4.

This research was financed by the Russian Foundation for Basic Research (07-01-00290) and the Programme for the Development of the Scientific Potential of Higher Schools (2.1.1/6194).

References

1. Contensou P. Couplage entre frottement de glissement et frottement de pivotement dans la theorie de la toupie. In: *Kreiselprobleme: Gyrodynamics, Symposium*. Berlin: Springer; 1963.
2. Karapetyan AV. *Stability of Steady Motions*. Moscow: Editorial URSS; 1998.
3. Karapetyan AV. Global qualitative analysis of the dynamics of the tippe top. *Izv Ross Akad Nauk MTT* 2008;**3**:33–41.
4. Leine RI, Gloker C. A set-valued force law for spatial Coulomb–Contensou friction. *Eur J Mech A* 2003;**22**(2):193–216.
5. Zhuravlev F. A model of dry friction in the problem of the rolling of rigid bodies. *Prikl Mat Mekh* 1998;**62**(5):762–7.
6. Smale S. Topology and mechanics. *Invent Math* 1970;**10**:4.

Translated by P.S.